Amplification of magnetic fields in non-rotating core collapse

Martin Obergaulinger, Thomas Janka, Oliver Just, Miguel Ángel Aloy

CAMAP, Departament d´Astronomia i Astrofísica, Universitat de València
Max-Planck-Institut für Astrophysik, Garching bei München

Supernovae and Gamma-Ray Burst in Kyoto, 2013-10-28 – 2013-11-01

Magnetic fields in core collapse

- magnetic fields need to be strong to have an effect on SNe
- But: stellar evolution theory predicts rather weak fields in the pre-collapse core

→ efficient amplification required

  - compression
  - linear winding by differential rotation
  - **hydromagnetic instabilities**: convection, magnetorotational instability (MRI), SASI

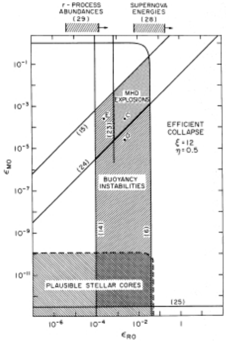

Meier et al., 1976

Magnetic fields in core collapse

	SASI	convection	MRI
energy mechanism	accretion flow advective-acoustic cycle	thermal buoyant transport of energy/species	diff. rotation magnetic transport of angular momentum
role of $\vec{b}$	passive; turbulent dynamo	passive; turbulent dynamo	instability driver; turbulent dynamo

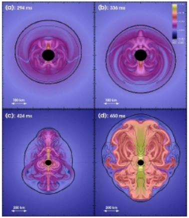

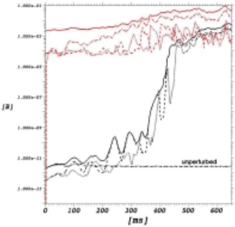

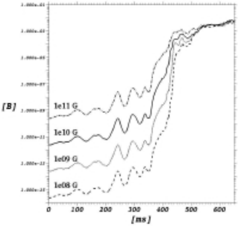

Endeve et al., 2008

The neutrino distribution

The ν field is equivalently described by its

- distribution function, $f(\vec{p}, \vec{x}, t)$, the probability to find a neutrino with a momentum $\vec{p}$ (i.e., energy $\epsilon = |\vec{p}|c$) at position $\vec{x}$, time t
- radiative intensity, $I(\vec{n}, \epsilon, \vec{x}, t)$, the energy carried by all ν of energy ϵ in direction $\vec{n} = \vec{p}/|\vec{p}|$ through a unit surface dA at position $\vec{x}$, time t

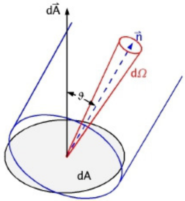

properties

- $f = \frac{(hc)^3}{c\epsilon^3} I$ is a relativistic invariant
- in local equilibrium with matter, f is given by the Fermi-Dirac distribution, $f_{\mathrm{FD}} = \frac{1}{\exp \frac{\epsilon - \mu_\nu}{k_{\mathrm{B}} T} + 1}$

The neutrino distribution

The ν field is equivalently described by its

- distribution function, $f(\vec{p}, \vec{x}, t)$, the probability to find a neutrino with a momentum $\vec{p}$ (i.e., energy $\epsilon = |\vec{p}|c$) at position $\vec{x}$, time t
- radiative intensity, $I(\vec{n}, \epsilon, \vec{x}, t)$, the energy carried by all ν of energy ϵ in direction $\vec{n} = \vec{p}/|\vec{p}|$ through a unit surface dA at position $\vec{x}$, time t

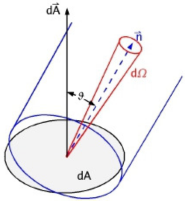

Boltzmann transport equation (mixed frame)

$$\begin{aligned}\partial_t I + \vec{n} \cdot \vec{\nabla} I &= \eta_0(\epsilon) - \chi_0(\epsilon) I \\ &+ \vec{n} \cdot \vec{v} \left(2\eta_0(\epsilon) - \epsilon \partial_\epsilon \eta_0 + [\chi_0(\epsilon) + \epsilon \partial_\epsilon \chi_0(\epsilon)] I\right)\end{aligned}$$

with advection, emission, absorption, and Doppler shift, aberration.

Radiation moments

Expand the intensity in angular moments, $M^{i_1 i_2 \dots i_m} = \int \mathrm{d}\vec{n} n^{i_1} n^{i_2} \dots n^{i_m} I$.

- 0^{th} moment: $E = \int \frac{\mathrm{d}\vec{n}}{4\pi} \left(\frac{\epsilon}{hc}\right)^3 f$, the energy density
- 1^{st} moment: $F^i = \int \frac{\mathrm{d}\vec{n}}{4\pi} \left(\frac{\epsilon}{hc}\right)^3 n^i f$, the momentum density
- 2^{nd} moment: $P^{ij} = \int \frac{\mathrm{d}\vec{n}}{4\pi} \left(\frac{\epsilon}{hc}\right)^3 n^i n^j f$, the pressure tensor
- etc. ad inf. (with no straightforward physical interpretation)

Moment equations

equation for the m^{th} moment contains the $(m+1)^{\text{th}}$ moment as a flux

$$\partial_t M^{i_1 \dots i_m} + \nabla_j M^{i_1 \dots i_m j} + \text{velocity terms} = S_m^{i_1 \dots i_m}$$

$\Rightarrow$ infinite series of equations $\equiv$ transport equation

Truncated moment system

evolve only the first 2 moments and obtain the higher (2^{nd} and 3^{rd}) moments by a local algebraic closure as a function of the lower moments

Truncated moment system

evolve only the first 2 moments and obtain the higher (2^{nd} and 3^{rd}) moments by a local algebraic closure as a function of the lower moments

0^{th} moment

assumption for the neutrino momentum

- free streaming: $\vec{F} = cE\vec{n}$; fails in optically thick regions
- diffusion: $\vec{F} = -\frac{c}{3\kappa}\vec{\nabla}E$; unphysical in vacuum
- flux-limited diffusion: ensure physical (not necessarily correct) vacuum limit $\Rightarrow$ parabolic equation

Truncated moment system

evolve only the first 2 moments and obtain the higher (2^{nd} and 3^{rd}) moments by a local algebraic closure as a function of the lower moments

1^{st} moment

set $P^{ij} = \frac{1-\chi}{2}\delta^{ij} + \frac{3\chi-1}{2}n^i n^j$ with a variable Eddington factor $\chi(E, \frac{|\vec{F}|}{cE})$.

- local approximation $\Rightarrow$ simpler and less expensive than Boltzmann solvers (but less accurate)
- genuinely multidimensional
- physical consistency: $\chi \to \{1/3, 1\}$ for $|\vec{F}|/(cE) \to \{0, 1\}$
- hyperbolic for suitable choice of χ

Neutrino interactions

Reactions with matter

- $n + \nu_e \rightleftharpoons p^+ + e^-$
- $p^+ + \bar{\nu}_e \rightleftharpoons n + e^-$
- $(A, Z) + \nu_e \rightleftharpoons (A, Z+1) + e^-$
- $n/p + \nu_X \rightleftharpoons n/p + \nu_X$
- $(A, Z) + \nu_X \rightleftharpoons (A, Z) + \nu_X$
- $e + \nu_X \rightleftharpoons e + \nu_X$
- $e^- + e^+ \rightleftharpoons \nu_X + \bar{\nu}_X$
- $N + N \rightleftharpoons N + N + \nu_X + \bar{\nu}_X$

- implementation following Rampp & Janka (2002)
- 2d simulations below neglect the reactions in grey

→ limited scope of our models

Tests

- homogeneous radiating sphere
- differentially expanding atmosphere
- neutrino transport in a post-bounce core
- spherical core collapse

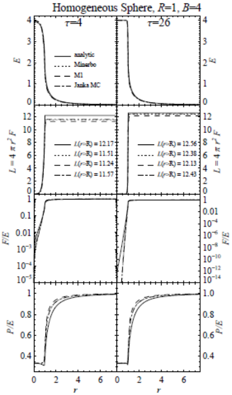

Figure 1. Comparison of the numerical results obtained using different closures with the analytic solution for the homogeneous sphere test problem. On the left (right) side the results for the case of moderate (high) opacity are plotted. The panels show from top to bottom the energy density, the luminosity, the flux factor and the Eddington factor against radius. In the second row the values of the (constant) luminosities outside of the sphere are given.

Tests

- homogeneous radiating sphere
- differentially expanding atmosphere
- neutrino transport in a post-bounce core
- spherical core collapse

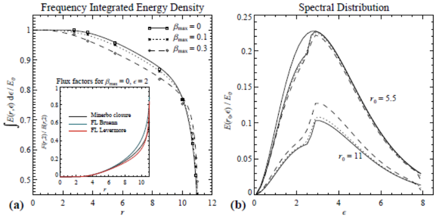

Figure 3. Results for the differentially expanding atmosphere. In Panel (a) the frequency integrated energy densities, normalized by $E_0 = \bar{E}(0)$, as function of radius are shown for different maximum velocities. The symbols denote the reference solution computed by Mihalas (1980). The inlet depicts the flux factor as obtained by our calculation for a specific energy-bin $\epsilon = 2$ where the radiation becomes optically thin at about $r = 5.5$. For comparison, we added the curves given by the flux-limiters, Eqs. (34), (35). In Panel (b) the spectral distributions of the normalized energy densities are shown for the same velocities at the two radii $r = 5.5, 11$ where the optical depth for the part $\epsilon < \epsilon_0$ of the spectrum is equal to 1 and ≈ 0, respectively. The thin solid line displays the equilibrium distribution $E^{eq}(\epsilon)$.

Tests

- homogeneous radiating sphere
- differentially expanding atmosphere
- neutrino transport in a post-bounce core
- spherical core collapse

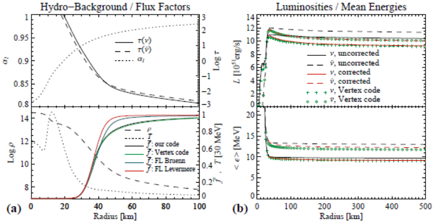

Figure 8. Comparison of the emission properties of the proto-neutron star at 300 ms post-bounce time on a fixed background with a dynamic reference calculation performed with the code VERTEX-PROMETHEUS including approximate general relativistic effects. In the top of Panel (a), we show the lapse function α_l and optical depths τ_ν. In the bottom panel, the density ρ, temperature T and mean flux factors $\bar f = \bar F/\bar E$ from both calculations are plotted. For comparison, we added the curves resulting from the flux-limiting prescriptions Eqs. (34), (35) applied to our profile of the energy density. In Panel (b), we depict the luminosities (top) and mean energies (bottom), both without and with the post-processing correction explained in the text. The green symbols denote results of the reference calculation, of which only every 10th grid point is regarded for better visualization. Note the different scaling of the abscissae in Panel (a) and Panel (b).

Tests

- homogeneous radiating sphere
- differentially expanding atmosphere
- neutrino transport in a post-bounce core
- spherical core collapse

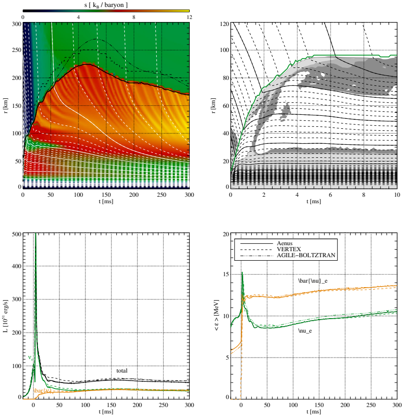

Tests

- homogeneous radiating sphere
- differentially expanding atmosphere
- neutrino transport in a post-bounce core
- spherical core collapse

Conclusion

in most regimes close to results of Boltzmann codes, but some limitations exist

Open issues

We want to study

- Where do the magnetic fields of young neutron stars come from?
- Under what conditions does the field amplification during a supernova explosion lead to dynamically important fields?
- How do the magnetic fields react back onto the flow?

But we are not aiming to answer

- Does a particular core produce a robust ν-driven SN explosion and, if so, how large is the explosion energy?
- How does the dynamics depend on the details of the equation of state and the neutrino physics?
- What are the consequences for nucleosynthesis?

Open issues

We want to study

- Where do the magnetic fields of young neutron stars come from?
- Under what conditions does the field amplification during a supernova explosion lead to dynamically important fields?
- How do the magnetic fields react back onto the flow?

But we are not aiming to answer

- Does a particular core produce a robust ν-driven SN explosion and, if so, how large is the explosion energy?
- How does the dynamics depend on the details of the equation of state and the neutrino physics?
- What are the consequences for nucleosynthesis?

Collapse of magnetised cores

- progenitor star: 15 $M_\odot$, solar metallicity
- no rotation $\rightarrow$ restricts possible field amplification mechanisms
- poloidal (off-centre dipole) magnetic fields of field strength $\leq 10^{12}$ G
- axisymmetric simulations
- spectral transport (16 energy bins) of ν_e and $\bar{\nu}_e$

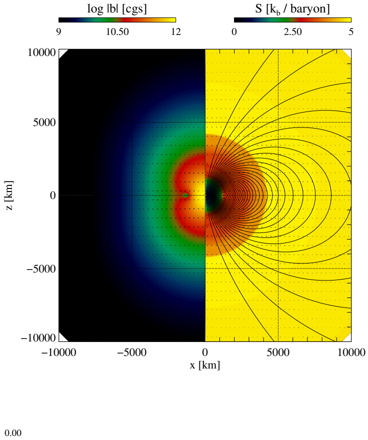

Field structure and entropy at $t = 0$

Overview

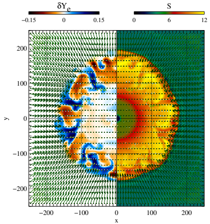

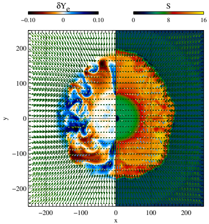

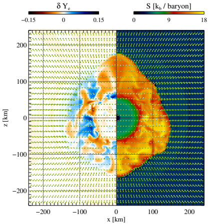

without magnetic field:
$\longrightarrow$ PNS convection, SASI and convection in the hot-bubble region

Overview

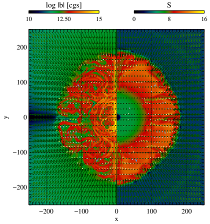

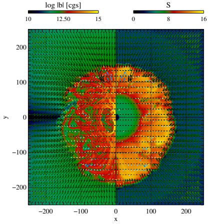

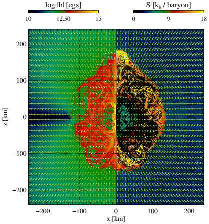

amplification of a weak field by compression, stretching and folding of field lines, and unstable Alfvén waves

Overview

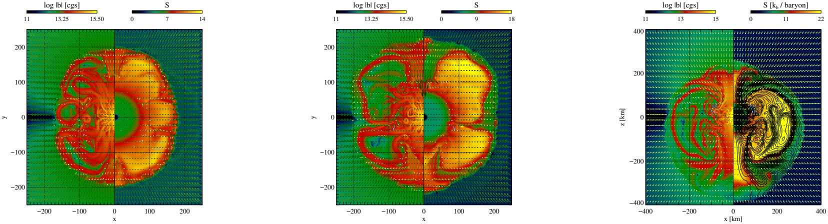

feedback of a strong field: field resists bending, slows down motion across field lines
→ modifies the growth of SASI, convection
→ development of very persistent large-scale patterns of upflows and downflows, stronger shock expansion

Field amplification

- most pronounced amplification occurs during collapse by compression
- for weak fields: significant increase in the hot-bubble on long time scales, caused by stretching and folding of field lines
- stronger initial fields experience less amplification, indicating dynamic feedback
- max. fields are magnetar-like

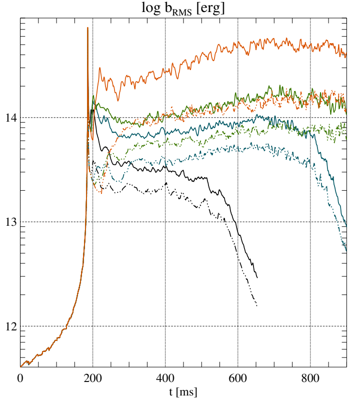

time evolution of the (rescaled) r.m.s. field strength: entire volume and hot bubble

Dynamic feedback

- feedback on the flow limit the amplification of stronger seed fields
- strong fields lead to much larger unstable modes and persistent downflows

$\rightarrow$ strong shock expansion

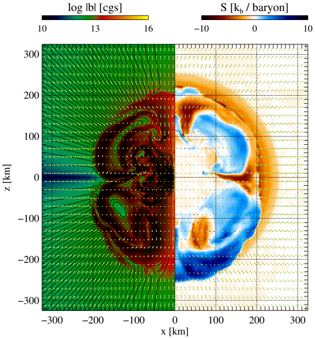

2d structure of a model with strong initial field

Dynamic feedback

- feedback on the flow limit the amplification of stronger seed fields
- strong fields lead to much larger unstable modes and persistent downflows

→ strong shock expansion

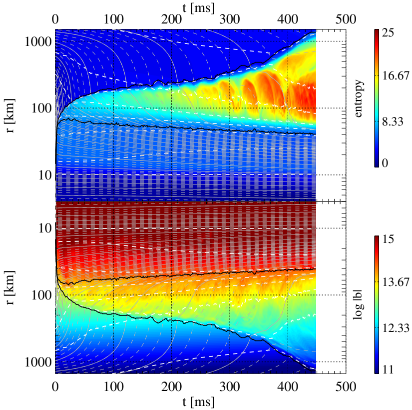

angularly averaged profiles of the strongest magnetised model as a function of time.

Summary

- the moment system with local closure is a good compromise between accuracy and effort
- we study the interplay of neutrino transport, hydrodynamics and magnetic fields, finding efficient amplification
  - compression
  - stretching by hydro instabilities

  and dynamic feedback
- next steps: switch on pair processes; rotating models